Poisson Models and Mean-Squared Error for Correlator Estimators of Time Delay

ALFRED O. HERO, MEMBER, IEEE, AND STUART C. SCHWARTZ, SENIOR MEMBER, IEEE

Abstract —A method for modeling large errors in correlation-based time delay estimation is developed in terms of level crossing probabilities. The level crossing interpretation for peak ambiguity leads directly to an exact expression for the probability of large error involving the hazard function associated with the level crossing process. Two models for the distribution of the error over the level crossing times yield approximations to the mean-square error (mse) which involve the low-order (< 4) finite dimensional distributions of the associated level crossing process. Application of an inhomogeneous Poisson model for the level crossings reduces the form of the approximations to a weighted sum of the Cramer–Rao lower bound and the second moment of a function of the level crossing intensity over time. Explicit expressions for the large error probability and the mse approximations are obtained under a Gaussian model for the correlator statistics. Analytical evaluation of the expressions, for the special case of flat low-pass observation spectra, indicate in a simple and unified manner properties of the correlator estimator which have been reported in previous studies. Qualitative and quantitative comparisons between these approximations and the Ziv–Zakai lower bound on estimation error are then presented. Finally, results of computer simulation are presented which indicate the accuracy of the approximations.

I. Introduction

A PERSISTENT problem in the design of multisensor array processing systems is the determination of the accuracy with which the spatial position of an energy emitting source can be estimated [9]. In the absence of noise the bearing angle of the source, relative to the baseline of a linear array, can be exactly determined by the time differences of arrival of the propagating wavefront between pairs of sensors. With a noise background the time differences of arrival, or time delays, must be estimated from the observed sensor waveforms.

For the two-sensor case the minimum achievable estimation error has been lower-bounded by the Ziv–Zakai lower bound (ZZLB) [21], [5]. For flat spectra and a sufficiently large observation-time signal-bandwidth product (BT), the simple correlator estimator has been shown to achieve the ZZLB. On the other hand, if BT is insufficiently large, the performance of the correlator estimator is known to fall short of the ZZLB [7]. In this case approximations to correlator error are of interest.

Manuscript received October 24, 1985; revised March 10, 1987. This work was supported in part by the Office of Naval Research under Contract N00014-81-K-0146 and by a 1985 Rackham Research Grant from the Graduate School of the University of Michigan, Ann Arbor. This paper was presented in part at the IEEE International Symposium on Information Theory, Brighton, England, June 1985.

A. O. Hero is with the Department of Electrical Engineering and Computer Science, University of Michigan, Ann Arbor, MI 48109.

S. C. Schwartz is with the Department of Electrical Engineering, Princeton University, Princeton, NJ 08544.

IEEE Log Number 8820322.

A simple and accurate approximation, the correlator performance estimate (CPE), was presented in [3] for the special case of flat observation spectra and moderately large BT. An extension of the CPE to bandpass spectra was presented in [7]. However, the computation appears impractical for small bandwidth signals due to the large number of sidelobes in the correlator trajectory.

We present a different technique to approximate correlator error based on a continuous time level crossing model for large error. The technique derives from the approximation of an upper bound on the mean-squared error (mse) obtained using the level crossing model. The principal advantage of this approach is that all input spectra can be treated in a unified manner via the intensity function of the associated correlator level crossing process.

We will deal with the following observation model. The outputs of two sensors, $x_1(t)$ and $x_2(t)$, are observed over a finite interval of time $t \in [0, T]$:

$$\begin{aligned} x_1(t) &= s(t) + n_1(t) \\ x_2(t) &= s(t-D) + n_2(t). \end{aligned} \tag{1}$$

The signal components, $s(t)$ and a delayed version $s(t-D)$, and the noises, $n_1(t)$ and $n_2(t)$, are zero-mean uncorrelated stationary Gaussian random processes. The delay D is restricted to an *a priori* region of possible delay $[-D_M, D_M]$. We assume the signal and noise spectia to have positive frequency support $\{f > 0: |f - f_0| < B/2\}$, where f_0 and B are the center frequency and the double-sided bandwidth of the signal process $s(t)$. The correlator estimator of D is implemented via estimation of the cross-correlation function $R_{12}(\tau)$ by the sample cross-correlation function, namely,

$$\hat{R}_{12}(\tau) \triangleq \frac{1}{T}\int_0^T x_1(t) x_2(t+\tau)\, dt. \tag{2}$$

The correlator estimator of time delay $\hat{D}$ is the location in time, within $[-D_M, D_M]$, at which the global maximum of the sample cross-correlation function occurs:

$$\hat{D} \triangleq \underset{\tau \in [-D_M, D_M]}{\operatorname{argmax}} \hat{R}_{12}(\tau). \tag{3}$$

An analytical expression governing the mse of the correlator estimator has been elusive due to the nonlinearity of the estimator as a function of the sensor outputs. In the

0018-9448/88/0300-0287$01.00

absence of such an exact expression, considerable effort has gone into constructing mse approximations. These can be divided into two general categories: local (or small error) mse approximations, and global mse approximations. If BT is sufficiently large, a small error approximation of estimator mse can be reliably applied for high SNR [6], [19]. The approximation is equivalent to the Cramer–Rao lower bound (CRLB). However, as the SNR decreases beyond a certain SNR threshold, which is BT dependent, the approximation is known to significantly underestimate the true global mse [3], [5], [7], [21]. This threshold occurs when the multiple peaks, or peak ambiguities, displayed by the correlation function over time, become of the same order of magnitude as the local peak occurring in the neighborhood of the true delay.

On the other hand, experiment has shown that the ZZLB is very nearly achieved by the correlator estimator for flat signal spectra and large BT. Hence in this case the ZZLB can be interpreted as an accurate approximation to the correlator mse. However, it has been established through simulation [7] and analysis [8] that the mse of the correlator estimator can significantly exceed the ZZLB for small BT.

The CPE [2] is a global mse approximation which accurately models the mse for spectrally flat lowpass signals and large BT [3]. The CPE is derived by modeling large error as the occurrence of exceedances of a random level by a set of independent identically distributed (i.i.d.) time samples of the trajectory over the *a priori* interval of delay. For the simple low-pass signal the i.i.d. samples and the random level referred to earlier are simply the output of the correlator at the zero locations of the delay-shifted signal autocorrelation function and the output at the true delay time, respectively. Thus the computation of the CPE involves the prespecification of a set of sample times for each case of observation spectra considered.

In an attempt to generalize the application of the CPE to the bandpass case, it was proposed in [7] to calculate the joint probability of level exceedance by the mutually correlated ambiguity-prone sidelobes of the correlator. The generalized CPE was shown to be a good approximation to the mse for the low center frequency-to-bandwidth ratio signal simulated in [7]. While application of the generalized CPE to large center frequency-to-bandwidth ratio was not discussed in [7], it is clear that as the center frequency-to-bandwidth ratio increases, the increased number of narrow sidelobes which need be considered would rapidly render the calculation of the joint probability of level exceedance impractical.

The CPE and generalized CPE can be interpreted as discrete-time mse approximations based on the computation of level exceedance probabilities. In what follows we will derive global mse approximations directly motivated by the continuous-time nonstationary nature of the sample cross-correlation function. In this approach the large error is characterized by the occurrence of level crossings rather than by level exceedances. The occurrence times of these level crossings play the same role in our approximation that the prespecified test points play in the definition of the CPE. This permits the direct application of our approximation to arbitrary spectra. Particularly for bandpass spectra, a level exceedance computation along the lines of [3], [7] involves the integration of a joint probability density whose definition is different for baseband and bandpass spectra and whose dimension is proportional to the center frequency-to-bandwidth ratio. On the other hand, the level crossing computation proposed here involves the integration of a bivariate joint density function: the intensity function of the level crossings.

II. Overview of Paper

The first step in our approximation is to separate the contributions of small errors and large errors to the overall mse. The second step is to relate the sequence of peak ambiguities to a sequence of level crossings associated with the sample correlation function. For this, the "ambiguity process" is defined whose zero exceedances occur in the neighborhood of the peak ambiguities and whose global maximum occurs at the global maximum of the correlator waveform.

Associating zero exceedances with zero crossings produces an exact expression for the probability of large error in terms of the hazard function of the zero crossing process. Also, conditioning the location of the global maximum of the ambiguity process on the occurrence times of its zero-exceeding local maxima gives an upper bound on the large-error mse. This is (26), involving the probability distribution of the global maximum over the set of local maxima. This is accomplished by bounding the occurrence times of local maxima with the occurrence times of a set of associated zero crossings.

The proposed class of mse approximations is generated by the assignment of various models for the probability distribution of the global maximum of the ambiguity function over the set of its local maxima and by the approximation of the small-error mse by the CRLB. Two such models are investigated here: 1) the "maximal model," Table II of Section III, which maximizes the mse over possible probability assignments, and 2) the "uniform model," Table III of Section III, which assigns equal likelihood to the local maxima. Under either of the two models the resulting expressions for mse, (29) and (30), respectively, involve the first-, second-, and third-order finite-dimensional distributions (fdd's) of the zero crossing process.

Next, some recent results concerning the representation of level crossing probabilities are discussed to motivate the approximation of the level crossing process by an inhomogeneous Poisson process. The inhomogeneous Poisson model can be regarded as a first-order approximation; it approximates the hazard function by the more tractable (incomplete) intensity function. In [4], [18] it was shown that the progressively "thinned" zero crossings converge in distribution to a Poisson process under some broad conditions. Based on a practical interpretation of this asymptotic result, we justify the Poisson level crossing model for high SNR and large BT. While useful bounds on the error in the Poisson approximation to the finite-dimensional distributions appear difficult to obtain, we provide a general nonparametric bound on the error in the Poisson approximation to the probability of large error. This bound indicates that, independent of BT, the Poisson error probability approximation is conservative under the asymptotic conditions of high and low SNR. Using the Poisson model, the mse bound under the maximal model (29) and under the uniform model (30) reduce to what will be called the maximal model Poisson (MMP) approximation (45), and the uniform model Poisson (UMP) approximation (47). These are linear combinations of the CRLB and a correction term for large errors. For the UMP the correction is the radius of gyration of the intensity function of the level crossing process.

To evaluate the UMP and MMP approximations, we apply a Gaussian model to the correlator output waveform and derive expressions for the intensity function of the zero crossing process as a function of sensor SNR. For flat low-pass signal spectra and large BT the intensity function is approximately independent of time, and the Poisson error probability and mse approximations reduce to an analytical form. It is noted that the UMP and MMP are identical when the intensity function of the zero crossings is small, i.e., for large SNR, and are indicative of an SNR threshold associated with a sudden onset of increasingly large errors.

Numerical comparisons between the UMP and MMP approximations, the ZZLB of [5], and computer simulations are presented for spectrally flat low-pass and bandpass sensor waveforms for various values of BT. To the extent that the cases studied are representative, the following results are obtained. The UMP correctly indicates the time delay estimate to be uniformly distributed over the *a priori* interval for exceedingly low SNR, while the MMP overestimates the mse by +5 dB over this region of SNR. Over the rest of the SNR range the MMP and UMP are virtually identical. The UMP and MMP behave similarly to the ZZLB, indicating multiple SNR thresholds of correlator performance. For the flat low-pass spectrum considered and large BT, the UMP approximation overestimates the actual mse, closely approximated by the CPE [3] for this case, by a maximum of approximately 5 dB. For a flat bandpass spectrum, in which case the actual mse exceeds the ZZLB by approximately 8 dB on the average, the UMP overestimates the mse by an average of less than 4 dB.

III. Estimation Errors and Level Crossings

Let $\hat{D}$ and D be the correlator estimate and the true delay parameter, respectively. Given a small positive constant δ, we separate the error $|\hat{D}-D|$ into small and large error regions $|\hat{D}-D| \le \delta$ and $|\hat{D}-D| > \delta$, respectively. An exact expression for the global mse results from direct application of the "law of total probability" to the mse $E\{(\hat{D}-D)^2\}$:

$$E\{(\hat{D}-D)^2\} = \sigma_{\text{loc}}^2(1-P_e) + \sigma^2 P_e \tag{4}$$

where

$$\sigma_{\text{loc}}^2 = E\{(\hat{D}-D)^2 | \hat{D}-D \in [-\delta, \delta]\} \tag{5}$$

$$\sigma^2 = E\{(\hat{D}-D)^2 | \hat{D}-D \notin [-\delta, \delta]\} \tag{6}$$

$$P_e = P(\hat{D}-D \notin [-\delta, \delta]) \tag{7}$$

are the conditional expectations of the squared error and the probability of large error, respectively.

While the expression (4) is valid for any definition of small-error region $\hat{D} \in [D-\delta, D+\delta]$, it will be convenient to choose δ such that σ_{loc}^2 is approximately equal to the CRLB, σ_{CRLB}^2 [6], when the CRLB is less than the maximal small-error mse δ^2. For flat spectra a standard asymptotic analysis gives, for large BT,

$$\sigma_{\text{loc}}^2 \le \min\{\sigma_{\text{CRLB}}^2 + o(\delta^2), \delta^2\} \tag{8}$$

where

$$o(\delta^2) \le \max_{D-\delta \le \xi \le D+\delta} |R_{SS}^{(3)}(\xi)| \sigma_{\text{CRLB}}^2 \delta^3.$$

In the sequel we will use the bound (8) with δ the smallest magnitude zero of the signal autocorrelation function: $\delta = 1/B$ for low-pass signals and $\delta = 1/4f_0$ for bandpass signals.

Next, we derive an expression for the large-error probability and develop an upper bound on the large-error mse, $\sigma^2 P_e$, based on a level crossing interpretation for large error. The occurrence of a peak equal or greater in magnitude than the maximum of the correlator within $[D-\delta, D+\delta]$ is called a peak ambiguity since it confounds the estimator's search for the location of the local maximum. The presence of peak ambiguities can be detected in two ways: by observing the values of the correlator output at the endpoints $-D_M, D_M$, and by detecting the occurrence of crossings of level zero by the difference between the correlator output over $[-D_M, D-\delta) \cup (D+\delta, D_M]$ and its local maximum in $[D-\delta, D+\delta]$. The conditional equivalence between the occurrence of level crossings and large error will be exploited to arrive at an exact expression for the large-error probability. On the other hand, the level crossings are not sufficient to give an exact expression for the large-error mse since the mse depends on the specific distribution of the peak ambiguity locations. By focusing on a subset of the level crossing locations, which constitute "candidates" for $\hat{D}$, a wide class of mse approximations can be generated. This is done by assignment of different probabilities to $\hat{D}$ over the set of candidates.

We first relate the occurrence of large errors to the occurrences of level crossings. Define the random level $l_\delta \triangleq \max_{u \in [D-\delta, D+\delta]} \hat{R}_{12}(u)$ and the "ambiguity process" $\Delta R(\tau) \triangleq \hat{R}_{12}(\tau) - l_\delta$. The level l_δ is the magnitude of the desired peak of the sample cross correlation, occurring near D (see Fig. 1). Note $\Delta R(\tau)$ must be negative over $\tau \notin [D-\delta, D+\delta]$ for no large error to occur. Next, define

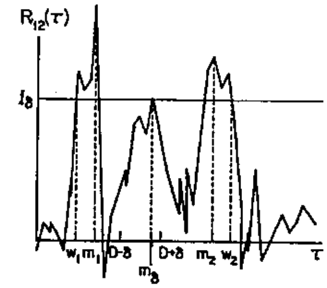

Fig. 1. Detection of global maximum of R_{12} over $[-D_m, D_m]$ gives correlator estimate of time delay $\hat{D} = m_1$. Local maxima occurrence times m_1 and m_2 are candidates for large error $\hat{D}$. Occurrence of level crossings of local maximum $l_\delta = \max_{u \in [-\delta,\delta]} R_{12}(u)$ by $R_{12}(\tau)$ at $\tau = w_1$ and $\tau = w_2$ implies occurrence of large error. Estimation of local maxima occurrence times by level crossing times upper-bounds error magnitude $|\hat{D} - D|$.

the level crossing counting process $N \triangleq \{N(\tau): \tau \in [-D_M, D_M]\}$ associated with the ambiguity process

$$N(\tau) \triangleq \begin{cases} N_u(-D_M, \tau), & \tau \in [-D_M, D-\delta) \\ N_u(-D_M, D-\delta), & \tau \in [D-\delta, D+\delta] \\ N_u(-D_M, D-\delta) + N_d(D+\delta, \tau), & \\ & \tau \in (D+\delta, D_M] \end{cases} \quad (9)$$

where $N_u(t_1, t_2)$ is the number of *up crossings* of zero by $\Delta R(\tau)$ over $\tau \in [t_1, t_2) \subset [-D_M, D-\delta)$, and $N_d(t_1, t_2)$ is the number of *down crossings* of zero by $\Delta R(\tau)$ over $\tau \in [t_1, t_2) \subset (D+\delta, D_M]$. If $\hat{R}_{12}$ is differentiable, an up crossing (down crossing) is defined as an intersection of zero by ΔR with a positive (negative) slope. For more general definitions see, for example, [12]. The process N is merely the running sum of the total number of up crossings to the left of the true delay plus down crossings to the right of the true delay (see Figs. 1 and 2).

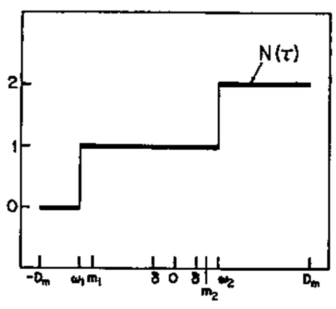

Fig. 2. Level crossing counting process N, defined in (9), for example of Fig. 1.

With the foregoing definitions, no large error occurs, i.e., $\hat{D} \in [D-\delta, D+\delta]$ if and only if 1) the boundary conditions $\Delta R(-D_M) < 0$ and $\Delta R(D_M) < 0$ are satisfied, and 2) $N(D_M) = 0$. For convenience, define the indicator random variables I_1 and I_2:

$$I_1 \triangleq \begin{cases} 1, & \text{if } \Delta R(-D_M) \geq 0 \\ 0, & \text{if } \Delta R(-D_M) < 0 \end{cases} \quad (10)$$

$$I_2 \triangleq \begin{cases} 1, & \text{if } \Delta R(D_M) \geq 0 \\ 0, & \text{if } \Delta R(D_M) < 0. \end{cases} \quad (11)$$

Hence the probability of large error is

$$P_e = 1 - P(N(D_M) = 0,\ I_1 = 0,\ I_2 = 0). \quad (12)$$

An important quantity associated with the counting process N is the hazard function λ:

$$\lambda(\tau) \triangleq \lim_{h \to 0} \frac{1}{h} P(N(\tau+h) - N(\tau) > 0 | N(\tau) = 0). \quad (13)$$

The hazard function is a measure of the probability that the first increment or point in N occurs at time τ. For the present application we will need the conditional hazards λ_{ij} given the boundary conditions $I_1 = i$, $I_2 = j$, $i, j = 0,1$:

$$\lambda_{ij}(\tau) \triangleq \lim_{h \to 0} \frac{1}{h} \cdot P(N(\tau+h) - N(\tau) > 0 | N(\tau) = 0,\ I_1 = i,\ I_2 = j). \quad (14)$$

As a matter of notation, subscripts "*" will denote averaging over the relevant index, e.g.,

$$\lambda_{i*}(\tau) \triangleq \lim_{h \to 0} \frac{1}{h} \cdot P(N(\tau+h) - N(\tau) > 0 | N(\tau) = 0,\ I_1 = i). \quad (15)$$

The hazard functions should not be confused with the (incomplete) intensities ρ and ρ_{ij} which are not conditioned on the past history of the process:

$$\rho(\tau) \triangleq \lim_{h \to 0} \frac{1}{h} P(N(\tau+h) - N(\tau) > 0) \quad (16)$$

$$\rho_{ij}(\tau) \triangleq \lim_{h \to 0} \frac{1}{h} P(N(\tau+h) - N(\tau) > 0) | I_1 = i, I_2 = j). \quad (17)$$

Under Leadbetter's regularity conditions [12], the intensity functions are related to the rate functions:

$$E_{ij}\{N(\tau)\} = \int_{-D_M}^{\tau} \rho_{ij}(u)\, du. \quad (18)$$

The following representation theorem associates the hazard function (14) and the probability of large error.

Theorem 1: Let $N \triangleq \{N(\tau): [-D_M, D_M]\}$ be the level crossing process defined in (9). If $(1/h)P(N(\tau+h) - N(\tau) > 0 | N(\tau) = 0;\ I_1 = 0,\ I_2 = 0)$ converges uniformly as $h \to 0$ to $\lambda_{00}(\tau)$, then

$$P_e = 1 - \exp\left\{-\int_{-D_M}^{D_M} \lambda_{00}(\tau)\, d\tau\right\} F(0,0) \quad (19)$$

where $F(x, y) \triangleq P(\Delta R(-D_M) < x;\ \Delta R(D_M) < y)$ is the left continuous joint probability distribution function associated with ΔR.

Proof: Fix $h > 0$ and let $t \in [-D_M, D_M]$. Define the partition $\{t_i\}_{i=1}^{p}$, of $[-D_M, t]$: $t_i \in [-D_M, t)$ and $t_{i+1} - t_i = h$. The event $N(t) > 0$ can be decomposed into the disjoint union $\bigcup_{i=1}^{p-1}\{N(t_{i+1}) - N(t_i) > 0 \cap N(t_i) = 0)\}$. Hence

$$P_{00}(N(t) > 0) \triangleq P(N(t) > 0 | I_1 = 0, I_2 = 0) = \sum_{i=1}^{p} \frac{1}{h} P_{00}(N(t_{i+1}) - N(t_i) > 0 | N(t_i) = 0) \cdot P_{00}(N(t_i) = 0) h. \tag{20}$$

Taking the limit as $h \to 0$, $p \to \infty$ yields, by uniform convergence of the Reimann sum,

$$P_{00}(N(t) > 0) = \int_{-D_M}^{t} \lambda_{00}(\tau)(1 - P_{00}(N(\tau) > 0))\, dt. \tag{21}$$

Equation (21) is an integral equation for the t-varying function $P_{00}(N(t) > 0)$ which has the unique solution $P_{00}(N(t) > 0) = 1 - \exp\{-\int_{-D_m}^{t} \lambda_{00}(\tau)\, d\tau\}$. The relation

$$P_e = 1 - P_{00}(N(D_m) = 0) F(0,0) \tag{22}$$

finishes the proof.

The foregoing theorem gives an exact representation of the probability of large error in terms of the hazard function associated with the level crossings. However, while the presence of level crossings is (conditionally) equivalent to the presence of ambiguity, the level crossings alone do not uniquely specify the location of the global maximum. On the other hand, the level crossings can be used to upper-bound the deviation of the location of the global maximum from the true delay D.

Given $N(D_M) = n$, let $w_1, \cdots, w_n$ be the points (times of increase) of the process $\{N(\tau): \tau \in [-D_M, D_M]\}$ defined in (9), and let $w_0 = -D_M$ and $w_{n+1} = D_M$. Specifically, define $w_1, \cdots, w_{n_u}$ the zero up crossings by ΔR to the left of D and $w_{n_u+1}, \cdots, w_n$ the zero down crossings to the right of D. Between each successive pair of up crossings and each successive pair of down crossings there is a local maximum constituting a peak ambiguity. The occurrence time of this maximum is a possible location for the correlator estimate $\hat{D}$. If $\Delta R(-D_M) > 0$, then the location of the maximum of ΔR between $-D_M$ and w_1 may also correspond to $\hat{D}$. Similar comments hold for the case $\Delta R(D_M) > 0$. Let $\{m_i\}_{i=0}^{n+1}$ be the set of locations of the local maxima

$$m_i \triangleq \begin{cases} \underset{\tau \in [-D_M, w_1]}{\operatorname{argmax}} \ \Delta R(\tau), & i = 0 \\ \underset{\tau \in [w_i, w_{i+1}]}{\operatorname{argmax}} \ \Delta R(\tau), & i = 1, \cdots, n_u - 1 \\ \underset{\tau \in [w_{n_u}, D-\delta]}{\operatorname{argmax}} \ \Delta R(\tau), & i = n_u \\ \underset{\tau \in [D+\delta, w_{n_u+1}]}{\operatorname{argmax}} \ \Delta R(\tau), & i = n_u + 1 \\ \underset{\tau \in [w_{i-1}, w_i]}{\operatorname{argmax}} \ \Delta R(\tau), & i = n_u + 2, \cdots, n \\ \underset{\tau \in [w_n, D_M]}{\operatorname{argmax}} \ \Delta R(\tau), & i = n + 1 \end{cases} \tag{23}$$

The contraction property of iterated expectations [20] relates the mean-squared error to the locations of the local maxima $\{m_i\}$:

$$\begin{aligned} E\{(\hat{D} - D)^2\} &= E\Big\{E\Big\{(\hat{D} - D)^2 | m_0, \cdots, m_{N(D_M)+1}, I_1, I_2, N(D_M)\Big\}\Big\} \\ &= E\Big\{(\hat{D} - D)^2 | I_1 = 0, I_2 = 0, N(D_M) = 0\Big\} \\ &\quad \cdot P(I_1 = 0, I_2 = 0, N(D_M) = 0) \\ &\quad + E\left\{\sum_{k=0}^{N(D_M)+1} (m_k - D)^2 P_k\right\} \end{aligned} \tag{24}$$

where P_i is the conditional probability that $\hat{D} = m_i$ given the random variables $I_1, I_2, N(D_M), \{m_i\}_0^{N(D_M)+1}$:

$$P_i \triangleq P\Big(\hat{D} = m_i | m_0, \cdots, m_{N(D_M)+1}, I_1, I_2, N(D_M)\Big). \tag{25}$$

Note that P_k is zero for all k if no large error occurs. Otherwise, $\Sigma_k P_k = 1$. It is also a given that if $\Delta R(-D_M) \le 0$ and $\Delta R(D_M) \le 0$, then $P_0 = 0$ and $P_{n+1} = 0$ since $\Delta R(m_0)$ and $\Delta R(m_{n+1})$ do not exceed zero. Define the *candidates* for $\hat{D}$ as the subset of $\{m_i\}$ for which a positive probability P_i may be assigned to each event $\hat{D} = m_i$. Note that $m_1, \cdots, m_n$ are always candidates, while m_0 and m_{n+1} may not be. The random variable P_i and the set of candidates are further specified in Table I.

TABLE I[a]

Candidate Locations for $\hat{D}$		I_1	I_2	N
$\underset{\tau \in [D-\delta, D+\delta]}{\operatorname{argmax}} \ \Delta R(\tau)$	$(P_0 = P_1 = 0)$	0	0	0
$m_1, \cdots, m_N$	$(P_0 = P_{N+1} = 0)$	0	0	> 0
m_1	$(P_0 = 0,\ P_1 = 1)$	0	1	0
$m_1, \cdots, m_{N+1}$	$(P_0 = 0)$	0	1	> 0
m_0	$(P_0 = 1,\ P_1 = 0)$	1	0	0
$m_0, \cdots, m_N$	$(P_{N+1} = 0)$	1	0	> 0
m_0, m_1		1	1	0
$m_0, \cdots, m_{N+1}$		1	1	> 0

[a]Set of candidates for location of global maximum of correlator under various conditions.

$I_1 \triangleq I[\Delta R(-D_M) > 0]$

$I_2 \triangleq I[\Delta R(D_M) > 0]$

$N \triangleq$ number of level crossings over $[-D_M, D_M] \triangleq N(D_M)$.

The obvious relation $|m_i - D| \le |w_i - D|$, $i = 0, \cdots, n+1$, and the identification of the first term on the left of the expression (24) as $\sigma_{\text{loc}}^2(1 - P_e)$, gives the upper bound on the mean-squared error:

$$E\{(\hat{D} - D)^2\} \le \sigma_{\text{loc}}^2 \exp\left\{-\int_{-D_M}^{D_M} \lambda_{00}(\tau)\, d\tau\right\} F(0,0) + E\left\{\sum_{k=0}^{N(D_M)+1} (w_k - D)^2 P_k\right\}. \tag{26}$$

The relation (26) is the basic result which relates the mean-squared error to the level crossing statistics. The result can be developed further via introduction of models for the probability distribution $\{P_i\}$.

Here we propose two models. The first model, $\{P_i^1\}$ in Table II, assigns all the probability mass to the candidate local maximum which maximizes the sum in (26) (maximal model). The second model, $\{P_i^2\}$ in Table III, assigns equal probability to all of the candidate local maxima m_i (uniform model).

TABLE II[a]

Maximal Model	I_1	I_2	N
$P_i^1=0$, For all i	0	0	0
$P_i^1=1$, $i=\operatorname{argmax}_{j=1,\cdots,N} \lvert w_j-D\rvert$	0	0	>0
$P_1^1=1$	0	1	0
$P_i^1=1$, $i=\operatorname{argmax}_{j=1,\cdots,N+1} \lvert w_j-D\rvert$	0	1	>0
$P_0^1=1$	1	0	0
$P_i^1=1$, $i=\operatorname{argmax}_{j=0,\cdots,N} \lvert w_j-D\rvert$	1	0	>0
$P_i^1=1$, $i=\operatorname{argmax}_{j=0,1} \lvert w_j-D\rvert$	1	1	0
$P_i^1=1$, $i=\operatorname{argmax}_{j=0,\cdots,N+1} \lvert w_j-D\rvert$	1	1	>0

[a] $P_i=P_i^1$ maximizes the mean-squared error over probability assignments to the events $\{m_i=\hat{D}\}$. Note $w_0=-D_M$ and $w_{N+1}=D_M$.

TABLE III[a]

Uniform Model	I_1	I_2	N
$P_i^2=0$, for all i	0	0	0
$P_i^2=\frac{1}{N}$, $i=1,\cdots,N$	0	0	>0
$P_1^2=1$	0	1	0
$P_i^2=\frac{1}{N+1}$, $i=1,\cdots,N+1$	0	1	>0
$P_0^2=1$	1	0	0
$P_i^2=\frac{1}{N+1}$, $i=0,\cdots,N$	1	0	>0
$P_i^2=\frac{1}{2}$, $i=0,1$	1	1	0
$P_i^2=\frac{1}{N+2}$, $i=0,\cdots,N+1$	1	1	>0

[a] $P_i=P_i^2$ assigns equal probability to events $\{m_i=\hat{D}\}$ over all candidates $\{m_i\}$.

Define the mse approximations under the previous models, mse_1 and mse_2:

$$\text{mse}_i = \sigma_{\text{loc}}^2 \exp\left\{-\int_{-D_M}^{D_M} \lambda_{00}(\tau)\,d\tau\right\} F(0,0) + E\left\{\sum_{k=0}^{N(D_M)+1} (w_k-D)^2 P_k^i\right\}, \qquad i=1,2. \tag{27}$$

Maximal Model

Partial expansion of the expectation to the right of (26) yields

$$\begin{aligned} E\left\{\sum_{k=0}^{N(D_M)+1}(w_k-D)^2P_k\right\} &= E_{00}\left\{\sum_{k=1}^{N(D_M)}(w_k-D)^2P_k\right\}P(I_1=0,\,I_2=0)\\ &+E_{01}\left\{\sum_{k=1}^{N(D_M)+1}(w_k-D)^2P_k\right\}P(I_1=0,\,I_2=1)\\ &+E_{10}\left\{\sum_{k=0}^{N(D_M)}(w_k-D)^2P_k\right\}P(I_1=1,\,I_2=0)\\ &+E_{11}\left\{\sum_{k=0}^{N(D_M)+1}(w_k-D)^2P_k\right\}P(I_1=1,\,I_2=1). \end{aligned} \tag{28}$$

In (28) E_{ij} denotes the conditional expectation given events $I_1=i$, $I_2=j$ for $i,j=0,1$. The summation indices for which P_k is conditionally zero have been suppressed as per Table I. Since each of the four terms in (28) can only be positive or zero, maximizing the individual expectations maximizes the entire sum. These expectations are in turn maximized by setting P_k equal to unity when k is the index of the maximum square deviation $(w_k-D)^2$, as indicated in Table II. Hence $E\{\Sigma(w_k-D)^2P_k\}$ is an upper bound on the large-error mse.

Referring to Appendix I, the equality in the following relation for mse_1 is established:

$$\begin{aligned} E\left\{(\hat{D}-D)^2\right\} &\le \text{mse}_1\\ &=\sigma_{\text{loc}}^2(1-P_e)+\int_{-D_M}^{D_M}(\tau-D)^2h_D(\tau)\,d\tau\\ &\quad+(D_M-D)^2\alpha_1+(D_M+D)^2\beta_1 \end{aligned} \tag{29}$$

where h_D, α_1, and β_1, given in (I.15) and (I.16), are functions of the fdd's: $\{P(N(\tau_1)\le k_1,\cdots,N(\tau_m)\le k_m)$: $\tau_i\in[-D_M,D_M]$, $k_i=0,1,\cdots\}$ up to order $m=3$.

Uniform Model

While the maximal model gives an upper bound on the mse, it may be excessively large at low SNR when the distribution of $\hat{D}$ is expected to be uniform over the *a priori* region. As an alternative, we consider the uniform assignment of probability $\{P_k\}$ over the indices of the four respective conditional expectations (28) (see Table III). In Appendix I the following expression is derived for the mse under the uniform model:

$$\text{mse}_2=\sigma_{\text{loc}}^2(1-P_e)+\int_{-D_M}^{D_M}(\tau-D)^2\rho(\tau)g_D(\tau)\,d\tau+(D_M-D)^2\alpha_2+(D_M+D)^2\beta_2. \tag{30}$$

In (30), α_2 and β_2 are decreasing functions of the probability that $\hat{R}_{12}(-D_M)$ and $\hat{R}_{11}(-D_M)$ exceed zero, respectively, and are decreasing functions of $P(N(D_M)>0)$:

$$\alpha_2 = E\left\{\frac{1}{N(D_M)+1}\middle| I_2=1\right\}E\{I_2\}$$

$$\beta_2 = E\left\{\frac{1}{N(D_M)+1}\middle| I_1=1\right\}E\{I_1\}.$$

The function $g_D(\tau)$ is defined as

$$g_D(\tau) \triangleq \sum_{n=1}^{\infty}\frac{1}{n}\sum_{k=1}^{n} a_{k-1,n-k}(\tau) \tag{31}$$

and we have defined the function

$$a_{k-1,n-k} \triangleq \lim_{h\to 0}\frac{1}{h}P\big(N(\tau)=k-1,\ N(\tau,D_M)=n-k \mid \cdot N(\tau+h)-N(\tau)>0\big). \tag{32}$$

$a_{l,k}$ can be interpreted as a "bidirectional" Palm measure which corresponds to the probability that, given the occurrence of a point at τ, this point is the kth occurrence in a sequence of n points occurring over $[-D_M, D_M]$. See [11] for a discussion of Palm measures.

Observe that the uniform model gives an upper bound on the mse under the following monotonicity condition on $\{P_i\}$: $|m_i - D| < |m_j - D|$ implies $P_i \geq P_j$. In other words, if the probability of a global maximum occurring at m_j decreases as the distance $|m_j - D|$ increases, then $E\{(\hat{D}-D)^2\} \leq \text{mse}_2$. However, even for simple models for the distribution of ΔR, e.g., Gaussian, it appears difficult to establish general sufficient conditions for monotonicity.

The expression for mse_1 (29) and mse_2 (30) are of similar form. Both consist of four terms. The first term is, as before, the small error contribution to the global variance. The second term is the contribution of the level crossing process, and the sum of the third and fourth terms is the contribution of any peak ambiguity which does not generate a level crossing (i.e., corresponding to the assignment $\hat{D} = \pm D_M$). Note that, as a function of the statistics of N, (29) and (30) behave in a manner expected from any reasonable mse approximation. In particular, as the probability that $N(D_M) > 0$ approaches zero, the hazards λ_{ij} must approach zero. For continuous $\hat{R}_{12}$, α_i and β_i will also typically approach zero. Hence in this case σ^2_{loc} dominates the expressions (29) and (30). Conversely, when $P(N(D_M)>0)$ becomes large, λ_{ij} becomes large and the second, third, and fourth large-error terms dominate.

The form of the expressions (29) and (30) is not sufficiently simple for computation. Indeed, while the intensity function ρ is straightforward to compute [12], the computation of the hazard function λ is generally difficult due to dependence between the increments of the point process N over time. However, when N is a Poisson process, the hazard function can be calculated easily.

IV. Poisson Models

The explicit evaluation of mse_1 and mse_2 depends on knowledge of the fdd's of N, the level crossing process associated with the ambiguity process ΔR. In this section we motivate the Poisson model for the random process N by the following: 1) as the intensity converges to zero over $[-D_M, D_M]$, N converges to zero at the same rate as a Poisson process converges to zero under a large BT assumption, 2) the Poisson model provides an upper bound on the probability $P(N(\sigma,\tau)>0)$, $\sigma,\tau \in [-D_M, D_M]$ in the limit of large and small intensity, and 3) if the ratio of the variance to the mean of N is bounded for large $E\{N\}$, the upper bound of 2) is also a lower bound.

Assume that $D = D_M$ so that N is the point process associated with the zero up crossings of ΔR over the *a priori* interval. It is easy to generalize the following discussion to the case of mixed up crossings and down crossings for a general D. We have established in [18] the following representation theorem for the up crossings generated by a random process $X \triangleq \{X(\tau)\}$ which will be applied to ΔR.

Theorem 2 [18]: Suppose the random process $X \triangleq \{X(\tau)\}$ has continuous sample functions with probability one, and let the joint density $f_{\tau_1,\tau_2}(x_1,x_2)$, of $X(\tau_1)$, $X(\tau_2)$ satisfy Leadbetter's conditions [12]. Then the probability $p(t) \triangleq P(N(\sigma,t)>0)$ of one or more up crossings of zero by X over the interval $[\sigma, t)$ satisfies the integral equation

$$p(t) = \int_\sigma^t \rho(\tau)(1-p(\tau))\,d\tau + Q(\sigma,t) \tag{33}$$

where

$$E\{N(\sigma,t)\} = \int_\sigma^t \rho(\tau)\,d\tau \tag{34}$$

and

$$\rho(\tau) = \lim_{h\to 0}\frac{1}{h}\int_0^\infty \eta f_{\tau,\tau+h}(0,\eta)\,d\eta. \tag{35}$$

In (35), $f_{\tau,\tau+h}(x, x+hy)$ is the joint density of $X(\tau)$ and $X(\tau+h)$ evaluated at the point $X(\tau)=x$ and

$$\frac{X(\tau+h)-X(\tau)}{h} = y.$$

The function $Q(\sigma,t)$ in (33) is the integral over $[\sigma,t]$ of the following measure of dependency between the forward increment $dN(\tau)$ and $N(\tau)$, denoted $q(\tau)$:

$$q(\tau)\,d\tau \triangleq P(dN(\tau)>0,\ N(\tau)=0) - P(dN(\tau)>0)P(N(\tau)=0). \tag{36}$$

Leadbetter's conditions, referred to in Theorem 2, are simple conditions on the second-order density of X such that the joint density of X and the right derivative of X at τ exists and has finite first moment. Theorem 2 gives an implicit relation for the probability that $N(\sigma,\tau)>0$. Although the intensity ρ is calculable in principle, the Q term in (33) is not known. It is conceivable that (33) may lend itself to an iterative solution if some increasingly good estimates of q are available. In so far as exact results are sought, however, the previous representation theorem may only be used as a verification method for some candidate for $P(N(\sigma,\tau)>0)$. On the other hand, Theorem 2 is useful for establishing some asymptotic results which will be outlined presently.

Unfortunately, there are but a few explicit distributional results for level crossings associated with a nontrivial random process X. To the best of our knowledge, published results exist only when X belongs to certain restricted classes of Markov or pseudo-Markov processes [13], [14]. On the other hand, there is a rich literature on the asymptotic distribution of level crossings for certain stationary random processes as the intensity approaches zero [15].

The most familiar asymptotic result takes the following form. Define a suitable sequence of increasingly high levels $\{l_m\}$. Given a stationary almost surely continuous random process X which satisfies some regularity conditions such as asymptotic mixing, the counting process N_m associated with the crossings by X of the increasingly high level l_m behaves increasingly like a (homogeneous) Poisson process. An equivalent interpretation is as follows: if μ_m and σ_m^2 are the mean and variance of X, the zero crossing process N_m approaches zero as a Poisson process when the "SNR" $|\mu_m/\sigma_m|$ converges to infinity.

In [18] an analogous but inhomogeneous Poisson limit for the zero crossings of a nonstationary process is shown. We will interpret this asymptotic result in a way which motivates the Poisson model for the zero crossings N of ΔR for large SNR. A heuristic argument for the Poisson limit follows based on Theorem 2.

Let the intensity $\rho=\{\rho(\tau)\}$ of the zero crossings by a random process X be sufficiently close to zero such that the crossings become rare events, i.e., with high probability the distance between successive crossing times is large. Furthermore, assume that X satisfies a "mixing condition" which guarantees the approximate independence of the trajectories of X over two distant disjoint intervals of time. Under the previous assumption, by virtue of their rarity, the zero crossings are approximately independent for small ρ. Specifically, for $p(t)=P(N(\sigma,t)>0)$, given $\epsilon>0$ for sufficiently small ρ, we have

$$|q(\tau)|<\epsilon\Big/\int_\sigma^t \exp\left(-\int_v^t \rho(u)\,du\right)dv, \qquad \sigma\le\tau\le t. \quad (37)$$

In this case (33) can be differentiated to yield the first-order differential equation

$$\frac{dp(t)}{dt}=\rho(t)(1-p(t))+q(t) \quad (38)$$

with initial condition

$$p(\sigma)=0. \quad (39)$$

Let $p^*(t)$ be the solution to (38) for $q(t)=0$. Then

$$p^*(t)=1-\exp\left\{-\int_\sigma^t \rho(\tau)\,d\tau\right\} \quad (40)$$

and the difference $\Delta \triangleq p^*-p$ satisfies the equation

$$\frac{d\Delta(t)}{dt}=-\rho(t)\Delta(t)-q(t) \quad (41)$$

with

$$\Delta(\sigma)=0.$$

From (41) and (37) the following bound is easily derived:

$$|p^*(t)-p(t)|\le\int_\sigma^t|q(\tau)|\exp\left(-\int_\tau^t\rho(u)\,du\right)d\tau<\epsilon. \quad (42)$$

Hence $N(\sigma,t)$ is within ϵ of having a Poisson distribution with rate $\int_\sigma^t\rho(\tau)\,d\tau$.

Equation (42) is valid for any interval $[\sigma,t)$. Consequently, by the approximate independent increment property of N the level crossings must closely approximate (in distribution) an inhomogeneous Poisson process with intensity ρ in the sense that for small δ,

$$P(N(t_0,t_1)=k_1,\cdots,N(t_n,t_{n+1})=k_n)$$
$$=\prod_{i=0}^n \frac{\left[\int_{t_i}^{t_{i+1}}\rho(\tau)\,d\tau\right]^{k_i}}{k_i!}\exp\left(-\int_{t_i}^{t_{i+1}}\rho(\tau)\,d\tau\right)+\delta. \quad (43)$$

The foregoing asymptotic result is made considerably more precise in [18]. Now let X of Theorem 2 be the ambiguity process ΔR of Section III. If ΔR can be accurately modeled by a Gaussian random process, then, conditioned on $\hat{R}_{12}(D)$, $\Delta R(\tau)$ and $\Delta R(u)$ are approximately independent for $|\tau-u|>1/B$. Assume BT $\gg 1$, and let ρ be sufficiently small so that $P(N(\tau,\tau+1/B)>0)<\epsilon$ for all τ.

With the foregoing, any two level crossings, i.e., increments of N, must be separated by a distance of at least $1/B$ with high probability. Therefore, for small ρ, or for what will be seen to be equivalent, large sensor SNR and large BT, the accuracy of the Poisson mse approximation is guaranteed by the convergence of the fdd's of N to a Poisson limit as in (43). The error in the Poisson approximation to the fdd's of N can be made explicit by a careful analysis of the "mixing parameter" for the ambiguity process and development of a relation between ϵ of (42) and δ of (43).

For large ρ the accuracy of the Poisson approximation to the finite-dimensional distributions of N is unknown. On the other hand, the form of the bound (42) suggests that the approximation error $\Delta(t)$ associated with the one-dimensional distribution $p(N(\sigma,t)>0)$ be small as $\rho\to\infty$ when q has less than exponential growth in ρ. A sufficient condition for

$$\lim_{E\{N(t)\}\to\infty}\Delta(t)=0$$

is

$$\lim_{E\{N(t)\}\to\infty}\frac{\operatorname{var}\{N(t)\}}{E\{N(t)\}}<\infty$$

(see [18]). Consequently, under the previous condition, the probability $P(N(t)>0)$ is well approximated by $1-\exp\{-E\{N(t)\}$ for asymptotically large or small mean rate of N.

The application of the Poisson model to the level crossing process N gives the following simple relation for the probability of large error (22):

$$P_e = 1 - e^{-E_{00}\{N(D_M)\}} F(0,0). \tag{44}$$

The mse approximations (29) and (30) become the following.

Maximal Model Poisson (MMP) Approximation ($D \geq 0$)

We have

$$\begin{aligned} \text{mse}_1 = \sigma_{\text{loc}}^2(1-P_e) &+ \int_{-D_M}^{D_M} (\tau - D)^2 z(\tau)\, d\tau \\ &+ (D_M - D)^2 e^{-E_{01}\{N(2D-D_M)\}} \\ &\cdot P(\Delta R(-D_M) < 0,\, \Delta R(D_M) \geq 0) \\ &+ (D_M + D)^2 P(\Delta R(-D_M) \geq 0) \end{aligned} \tag{45}$$

where

$$\begin{aligned} z(\tau) \triangleq \rho_{00}(\tau)\Big[& e^{-E_{00}\{N(2D-\tau,\tau)\}} I_{[D,D_M]}(\tau) \\ &+ e^{-E_{00}\{N(\tau,2D-\tau)\}} I_{[2D-D_M,D]}(\tau)\Big] \\ &\cdot e^{-E_{00}\{N(D_M)\}} F(0,0) \\ &+ \rho_{0\bullet}(\tau) e^{E_{0\bullet}\{N(\tau)\}} I_{[-D_M,2D-D_M]}(\tau) \\ &\cdot P(\Delta R(-D_M) < 0). \end{aligned} \tag{46}$$

Uniform Model Poisson (UMP) Approximation

We have

$$\begin{aligned} \text{mse}_2 \leq \sigma_{\text{loc}}^2(1-P_e) & \\ &+ \int_{-D_M}^{D_M} (\tau - D)^2 \hat{\rho}(\tau)\, d\tau \left(1 - e^{-E\{N(D_M)\}}\right) \\ &+ (D_M - D)^2 \frac{1 - e^{-E_{\bullet 1}\{N(D_M)\}}}{E_{\bullet 1}\{N(D_M)\}} P(\Delta R(D_M) \geq 0) \\ &+ (D_M + D)^2 \frac{1 - e^{-E_{1\bullet}\{N(D_M)\}}}{E_{1\bullet}\{N(D_M)\}} P(\Delta R(-D_M) \geq 0). \end{aligned} \tag{47}$$

In (47) we have defined the normalized intensity

$$\hat{\rho}(\tau) \triangleq \rho(\tau) \Big/ \int_{-D_M}^{D_M} \rho(u)\, du. \tag{48}$$

To obtain (44)–(47), we have used the fact that under the Poisson model the hazards λ (13) and λ_{ij} (14) are identical to the intensities ρ (16) and ρ_{ij}(17), respectively, due to the Poisson independent increment property [11]. Furthermore, the function $h(\tau)$ (31) reduces to the expression

$$h(\tau) = \frac{P(N(D_M) > 0)}{E\{N(D_M)\}}. \tag{49}$$

Note that in the limit of large intensity ρ the MMP converges to the worst case mse of $\max\{(D_M - D)^2, (D_M + D)^2\}$ while the UMP converges to the mse of a uniform distribution $D_M^2/3 + D^2$. Regarding the UMP approximation (47), we note that as the intensity ρ increases, the UMP discounts the small-error mse, σ_{loc}^2 by P_e, and adds an increasingly large quantity. This quantity represents the mean-squared deviation of the peak ambiguities. In the next section we present results of the numerical evaluation of the expressions (45) and (47) which show the UMP to be virtually identical to the MMP except for large ρ.

V. Applications

In this section we will explicitly calculate the intensities under a Gaussian assumption and investigate the resulting form of the Poisson mse approximations for simple lowpass and bandpass signals and the case of zero delay $D = 0$. We make the following assumptions: a) $\hat{R}_{12}$ is a Gaussian random process with nonstationary mean and analytic covariance function, and b) $\max_{u \in [-\delta,\delta]} \hat{R}_{12}(u) = \hat{R}_{12}(0)$. The Gaussian model invoked by assumption a) is reasonable for large BT. In this case the sample cross-correlation function represents the average of a large number of independent identically distributed random processes over subintervals of $[0,T]$, each of length $1/B$. Since the exceedance of $\hat{R}_{12}(0)$ by $\hat{R}_{12}(\tau)$ for some $\tau \in [-D_M, D_M] - [-\delta, \delta]$ does not necessarily imply a peak ambiguity, assumption b) is pessimistic at worst.

In the particular case $D = 0$ and $\text{BD}_M \gg 1$, the symmetry of the intensities and the approximate independence between $\Delta R(D_M)$ and $\{\Delta R(\tau)\colon \tau \in [-D_M, \delta]\}$ give simplified expressions for (45) and (47):

$$\begin{aligned} \text{mse}_1 = \sigma_{\text{loc}}^2(1-P_e) & \\ &+ 2\int_{-D_M}^{0} \tau^2 \rho_{1\bullet}(\tau) \exp\left(2\int_{-|\tau|}^{0} \rho_{1\bullet}(u)\, du\right) d\tau \\ &\cdot \exp\left(-2\int_{-D_M}^{0} \rho_{0\bullet}(\tau)\, d\tau\right) F(0,0) \\ &+ D_M^2(1 - F(0,0)) \end{aligned} \tag{50}$$

$$\begin{aligned} \text{mse}_2 = \sigma_{\text{loc}}^2(1-P_e) & \\ &+ 2\int_{-D_M}^{0} \tau^2 \hat{\rho}(\tau)\, d\tau \left(1 - \exp\left(-2\int_{-D_M}^{0} \rho(\tau)\, d\tau\right)\right) \\ &+ 2D_M^2 \frac{1 - \exp\left(-2\int_{-D_M}^{0} \rho_{1\bullet}(\tau)\, d\tau\right)}{2\int_{-D_M}^{0} \rho_{1\bullet}(\tau)\, d\tau} \\ &\cdot P(\Delta R(D_M) \geq 0) \end{aligned} \tag{51}$$

where

$$P_e = 1 - \exp\left(-2\int_{-D_M}^{0} \rho_{0\bullet}(\tau)\, d\tau\right) F(0,0). \tag{52}$$

Explicit formulas for ρ, $\rho_{0\bullet}$, and $\rho_{1\bullet}$ can be derived for

$\tau \leq 0$ by using assumptions a) and b) (Appendix II):

$$\rho_{0\cdot}(\tau) = \begin{cases} K_1 \int_0^{\infty} y\Phi(a_0 y + a_1)\phi(y + a_2)\, dy, & \tau \leq -\delta \\ 0, & -\delta < \tau \leq 0 \end{cases}$$

$$\rho(\tau) = \begin{cases} K_2\phi(a_3)[\phi(a_4) + a_4\Phi(a_4)], & \tau \leq -\delta \\ 0, & -\delta < \tau \leq 0 \end{cases} \tag{53}$$

$$\rho_{1\cdot}(\tau) = \frac{\rho(\tau) - P(\Delta R(-D_M) < 0)\rho_{0\cdot}(\tau)}{P(\Delta R(-D_M) > 0)}. \tag{54}$$

Here $K_1, K_2, a_0, \cdots, a_4$ are functions of τ given in Appendix II. The functions Φ and ϕ are the standard Gaussian distribution and density, respectively.

For large BD_M, small δ, and flat low-pass signal and noise spectra of bandwidth B and magnitudes S and N, respectively, it can be shown [4] that the intensities ρ and $\rho_{\cdot 0}$ of (53) are essentially independent of time and are virtually identical in functional form. The unconditional average number of zero crossings $E\{N(D_M)\}$ takes the form

$$E\{N(D_M)\} = 2\rho D_M = \frac{BD_M}{\sqrt{3}\sqrt{2 + |\gamma_{12}|^2}}\phi(\gamma'\sqrt{BT}). \tag{55}$$

$|\gamma_{12}|$ is the magnitude coherency between x_1 and x_2, $|\gamma_{12}| \triangleq S/(S+N)$, S/N is the SNR, and we have defined $\gamma' = |\gamma_{12}|/\sqrt{2 + |\gamma_{12}|^2}$. The MMP and UMP approximations (45) and (47) become particularly simple to evaluate:

$$\begin{aligned} \text{mse}_1 = {} & \sigma_{\text{loc}}^2 e^{-E\{N(D_M)\}}\Phi^2(\beta) \\ & + D_M^2\left[1 - 2\frac{e^{-E\{N(D_M)\}} - 1 + E\{N(D_M)\}}{E^2\{N(D_M)\}}\right] \\ & \cdot\Phi^2(\beta) + D_M^2[1 - \Phi^2(\beta)] \end{aligned} \tag{56}$$

and

$$\begin{aligned} \text{mse}_2 = {} & \sigma_{\text{loc}}^2 e^{-E\{N(D_M)\}}\Phi^2(\beta) \\ & + \frac{D_M^2}{3}\left(1 + \frac{3}{E\{N(D_M)\}}[1 - \Phi^2(\beta)]\right) \\ & \cdot(1 - e^{-E\{N(D_M)\}}) \end{aligned} \tag{57}$$

where

$$\beta = -E\{\Delta R(-D_M)\}\Big/\sqrt{\text{var}\{\Delta R(-D_M)\}}.$$

Some general comments concerning the behavior of mse_1 and mse_2 can now be made based on (55)–(57). First, as the coherency increases to one (high SNR) the average number of level crossings approaches zero and β goes to positive infinity. Hence one can verify that under these conditions,

$$\text{mse}_1 \approx \text{mse}_2 \approx \sigma_{\text{loc}}^2 e^{-E\{N(D_M)\}} + \frac{D_M^2}{3}E\{N(D_M)\}. \tag{58}$$

On the other hand, decreasing the coherency (low SNR) causes an increase in ρ, and hence both mse_1 and mse_2 increase to D_M^2 and $D_M^2/3$, respectively. Second, the term $\phi(\gamma'\sqrt{BT})$ displays an abrupt increase in magnitude as the SNR decreases beyond a BT-dependent threshold SNR_t (SNR_t is such that $\gamma'\sqrt{BT} \approx 3$), resulting in a sudden increase in the rate $E\{N(D_M)\}$. In general, increasing BT decreases SNR_t, expanding the SNR range of error-free operation of the correlator. Finally, the quantity BD_M governs the steady-state value of the average number of level crossings as the SNR decreases to zero. Increasing the length of the *a priori* region $[-D_M, D_M]$ naturally makes large errors more likely.

The behavior of the MMP and UMP approximations as a function of SNR is analogous to the behavior of the ZZLB reported in [5] for low-pass signals, with the following exception. Consider the asymptote of (55) as SNR approaches infinity. In this case $|\gamma_{12}| \to 1$ and

$$E\{N(D_M)\} \to \frac{BD_M}{\sqrt{6}}\phi(k_1\sqrt{BT}) \tag{59}$$

where k_1 is a finite numerical constant. This interesting result implies that even at infinite SNR, large errors (level crossings) may be committed. This is in agreement with results obtained in [8], showing the suboptimality of the correlation estimate of delay except for very large BT.

Fig. 3 is a plot of the intensity surface as a function of input SNR and time for a flat low-pass signal spectrum of single-sided bandwidth, $B = 100$ Hz. The observation time was set to $T = 8$ s. The time window displayed in the figure extends across the first few sidelobes of the autocorrelation function of the signal, starting at $\delta = 1/B$ (at the northeast corner of Fig. 3 for an SNR of 0 dB). In the figure the global maximum of the signal autocorrelation function lies beyond the rightmost point on the t axis. Note the abrupt increase of the intensity near the SNR threshold indicated by SNR_t on Fig. 3. At low SNR the intensity surface saturates (average height is about 4.5 ambiguities per unit time) with only a small ripple variation over time. For high SNR the intensity is essentially zero uniformly over the time window. In the intermediate range of SNR (approximately −8 to −20 dB), the average number of peak ambiguities per unit time is higher in the neighborhoods of the local maxima of the signal autocorrelation than in the outlying regions.

In Fig. 4 the intensity surface is displayed for a band-pass signal at center frequency $f_0 = 500$ Hz with band-

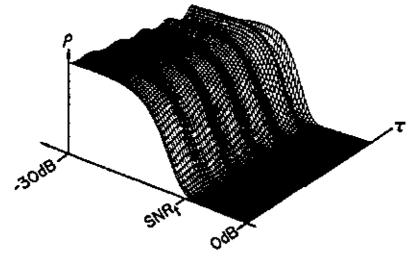

Fig. 3. Intensity surface for low-pass signal over time and SNR.

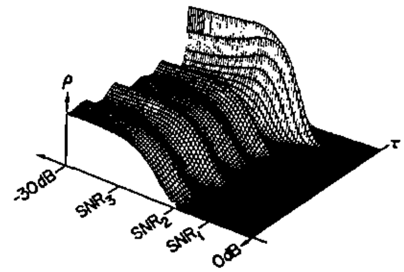

Fig. 4. Intensity surface for bandpass signal over time and SNR.

width $B=200$ Hz and $T=8.0$ s. Here the time window extends from the first zero crossing of the autocorrelation function of the signal $\delta=1/4f_0$ to approximately the fifth sidelobe away from the origin. Fig. 4 is oriented identically to Fig. 3 for the lowpass case; the global maximum of the autocorrelation is beyond the rightmost point on the t axis. Contrasting Fig. 4 with Fig. 3, it is evident that the variation in the intensity surface is much more severe in the bandpass case, even at low SNR. In fact, the average number of peak ambiguities is orders of magnitude greater near the first sidelobe than over the rest of the time axis. A distinctive feature of Fig. 4 is the SNR difference between the point SNR_1, where a rapid rise in the intensity of ambiguity first begins (in the region of the first sidelobe) and the point SNR_2, where a uniform increase of the ambiguity over time is evident. This implies the existence of at least two separate SNR thresholds in the bandpass case.

In [5], four distinct regions of performance were discovered based on a study of the Ziv–Zakai lower bound for the simple bandpass spectra considered. These regions are delineated by two SNR thresholds, SNR_1 and SNR_2, and an SNR point, SNR_3, beyond which only *a priori* information is useful. In light of the present results displayed in Fig. 4, a physical explanation of the threshold phenomenon in terms of the intensity function of the level crossing can be proposed. A similar explanation is presented in [21], based on the behavior of the ZZLB.

It may be helpful to refer to Fig. 5(a) and (b) in interpreting the following comments. For SNR larger than SNR_1, the only significant source of errors comes from small variations in the maximum of the narrow peak, which occurs at the true delay. As the SNR approaches SNR_1, however, a rapid increase in the error occurs because of the proximity of the maxima of the closely spaced high-frequency sidelobes of the signal autocorrelation.

Due to rapid attenuation of the high-frequency component by the autocorrelation envelope (see Fig. 5(b)) an initial saturation of the errors occurs within the central lobe of the envelope as the SNR approaches SNR_2. The occurrence of additional large errors over the outlying remainder of the *a priori* interval is precluded until a sufficiently low second threshold is attained, SNR_2.

Beyond SNR_2 the outlying ambiguity becomes as significant as that falling within the central lobe of the envelope, and the error begins a second episode of rapid

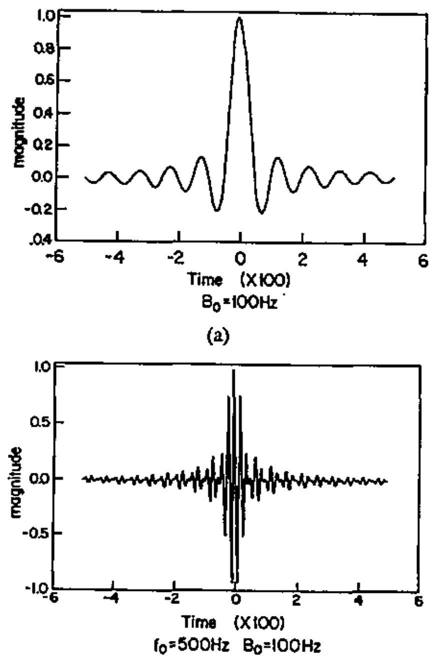

Fig. 5. Signal autocorrelation function. (a) For spectrally flat low-pass signal. (b) For spectrally flat bandpass signal.

increase. This increase continues until total saturation of the *a priori* interval is achieved at SNR_3.

Beyond SNR_3 a limit on the number of ambiguities is imposed by the maximum number of times a waveform of finite bandwidth B can undergo zero crossings within the *a priori* region. While SNR_3 is not really a threshold in the sense of SNR_2 and SNR_1, we will refer to all three as SNR thresholds.

For comparison with the results of a simulation of the correlator for low-pass signals performed in [3], we generated plots of the MMP and UMP approximations (56) and (57), the ZZLB [5], the CRLB [10], and the CPE [2] as a function of SNR for $BT=1600$ and $BD_M=25$. Fig. 6

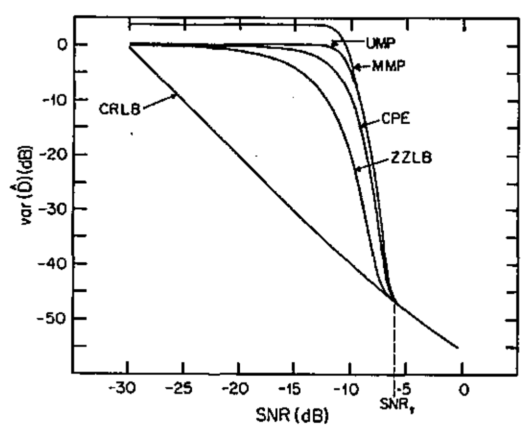

Fig. 6. Comparison of Poisson MSE approximations, MMP and UMP, with CPE, ZZLB, and CRLB for signal with flat lowpass spectrum. $BT=1600$, $BD_m=25$, and $D=0$.

shows the results of this numerical comparison. Note the presence of an SNR threshold, SNR_t, displayed by all but the CRLB in the neighborhood of -6 dB. The MMP and UMP approximations are essentially identical except at very low SNR and are uniformly larger than the lower bounds and the CPE. This confirms the conservatism of the Poisson approximation for this case.

In [3] the CPE for this example was compared to the simulated performance of the correlator. In that study the CPE matched the simulated mse to within about 2 dB on the average. Hence for the low-pass large BT case considered here, the UMP is less accurate as an mse approximation than the CPE by a maximum of about 4 dB.

We numerically evaluated the integrals in (45), (47), and (53) for a spectrally flat bandpass signal with center frequency to bandwidth ratio $f_0/B=10$, and $BD_M=25$. The results are plotted in Figs. 7 and 8, along with plots of the CRLB and ZZLB, for BT = 200 and BT = 80, respectively. Again, the MMP and UMP approximations are virtually identical over the majority of the range of SNR, differing by a maximum of only 5 dB at low SNR. They behave similarly to the ZZLB in Fig. 7, indicating the presence of three distinct SNR thresholds (e.g., SNR_{t1}, SNR_{t2}, and SNR_{t3} in Fig. 7) of performance. For $\mathrm{SNR} < \mathrm{SNR}_{t1}$ the MMP and UMP approximation becomes a much better predictor of mse than the CRLB. $[\mathrm{SNR}_{t2}, \mathrm{SNR}_{t1}]$ is a region where, with high probability, large errors are concentrated in the interval $\hat{D} \in [-1/B, 1/B]$. When $\mathrm{SNR} < \mathrm{SNR}_{t2}$, the error approaches that of a uniform random variable over $[-D_M, D_M]$; the estimate $\hat{D}$ is useless. For BT = 80 (see Fig. 8) the MMP and UMP approximations have moved away from the ZZLB relative to BT = 200. Indeed, they appear to hit an asymptote with increasing SNR; the correlator commits large errors even as the SNR approaches infinity. As in the case of low-pass signals, this corroborates the reported suboptimality of the correlator estimate for small BT [7], [8].

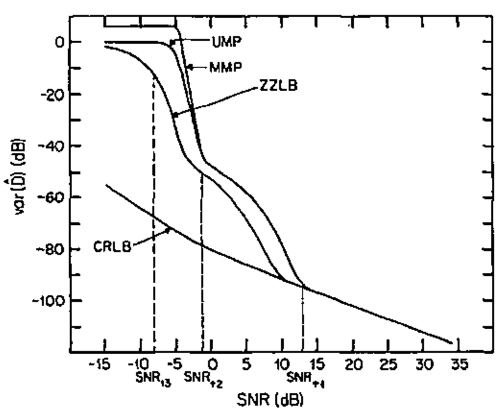

Fig. 7. Comparison of UMP and MMP with ZZLB and CRLB for bandpass signal spectrum. $f_0/B=10$, $\mathrm{BD}_m=25$, BT = 200, and $D=0$.

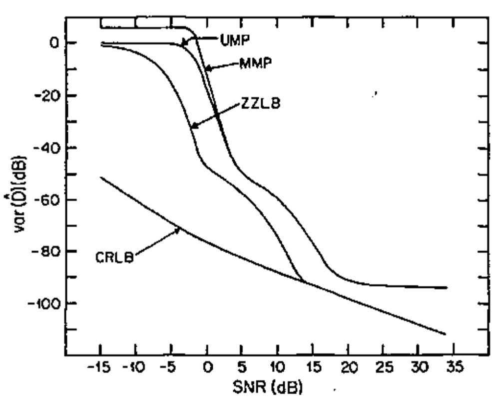

Fig. 8. Comparison of UMP and MMP with ZZLB and CRLB for bandpass signal spectrum. $f_0/B=10$, $\mathrm{BD}_m=25$, BT = 80, and $D=0$.

Finally, a discrete-time simulation of the correlator estimator was performed for bandpass signal and noise spectra and low BT. The relevant parameters chosen for the simulation are $f_0/B=2.5$, BT = 50, and $\mathrm{BD}_M=8$ and $D=0$. The details of the simulation procedure are now described. For SNR values of -8, -4, 0, 4, and 12 dB, 9000 Gaussian white noise sequences of length 4096 were generated using a standard pseudonoise generator and a Box–Muller transformation. Then bandpass waveforms of length 4096 were obtained by truncating all but a narrow band of indices in the fast Fourier transforms (FFT's) of the white noise sequences. Successive groups of three waveforms were then combined to form sensor waveforms x_1 and x_2 of (1).

Finally, a set of 3000 correlator estimates were generated by detecting the global peak of the output of the discrete time version of (2), and the sample mse was calculated along with 95-percent confidence intervals. Fig. 9 displays the results of the simulation. The vertical dimension of the Φ characters in the figure indicate the 95-percent confidence interval for the actual mse. Plotted for comparison are the CRLB, ZZLB, and UMP approximations. The combination of the ZZLB and the UMP approximations appears to bound the range of simulated mse.

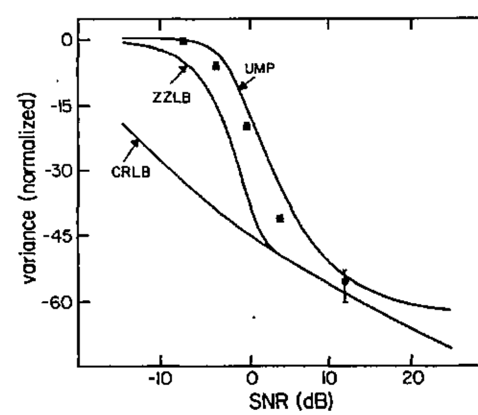

Fig. 9. Comparison of UMP with ZZLB and simulation for $f_0/B=2.5$, $\mathrm{BD}_m=8$, BT = 50, and $D=0$.

On the average, below an SNR of 5 dB, the true mse is significantly closer to the UMP than it is to the ZZLB. Note in particular that at SNR $= -8$ dB, the UMP is within the 95-percent confidence interval of the true mse while the ZZLB is quite loose at this SNR by about 5 dB. On the other hand, at SNR $= 4$ dB the mse is approximately equidistant from the UMP and ZZLB by approximately 7 dB.

VI. Conclusion

A method for modeling large errors in correlator time-delay estimators was developed in terms of level crossing probabilities. The level crossing interpretation for peak ambiguity led directly to an exact expression for the probability of large error involving the hazard function associated with the level crossing process. The mse of the time delay estimate was then considered under the aforementioned large-error model. An upper bound on the large-error mse was derived, and a class of large-error mse approximations was introduced via a class of models for the distribution of the erroneous estimate $\hat{D}$ over the level crossing times. Two models were presented: a bound-preserving maximal model and a uniform model.

A Poisson approximation to the level crossings was then presented which was motivated by a representation theorem. The Poisson approximation was then applied to the large-error approximations to derive simple expressions for the global mse of the correlator estimate, the MMP and UMP approximations (45) and (47). These approximations involve certain conditional (incomplete) intensity functions of the level crossing process. Under a Gaussian model for the sample cross-correlation trajectory, explicit expressions for the intensity functions were derived. For low-pass signal spectra and large BT, our approximations reduced to analytic forms (56) and (57). Investigation of the behavior of (56) and (57) revealed, in a unified manner, the importance of several factors on correlator performance reported throughout the time delay estimation literature, e.g., [2], [3], [5], [7], and [8]. The MMP and UMP approximations were then compared against the ZZLB for typical examples of low-pass and bandpass signals via numerical integration. The results show that the UMP is close to the MMP over the majority of the SNR region studied, suggesting that the uniform model is bound preserving over this range.

For simple low-pass spectra and large BT, the UMP and MMP appear to overestimate the true mse for which the CPE [3] is more accurate. Likewise, for the simple low *center frequency-to-bandwidth* ratio bandpass case studied in [7] the approximation method of [7] appears more accurate. The degree to which the UMP and MMP overestimate the mse for more complicated spectra than the simple cases considered here is unknown at present. For such spectra the methods of [3] and [7] also are inapplicable or difficult. On the other hand, the technique is quite powerful in that a large class of approximations are possible through the application of different models to the $\{P_i\}$ in (26) and to the point process N (9).

There are several future directions for study. One is to extend the upper bound (26) on the large error mse we have developed in Section III to a lower bound. A straightforward modification of our procedure for upper-bounding the distance between the local maxima occurrence times and the true delay using up crossing and down crossing occurrence times yields lower bounds on the large-error mse by exchanging the roles played by the up crossing and down crossing occurrence times. The upper and lower bounds can then be interpreted as a description of a confidence region for the mse.

It is known that for a small average number of level crossings the Poisson model is accurate; it preserves the upper bound (29). In the interest of finding analytic bounds on correlator mse, bound-preserving level crossing distributions should be investigated.

In its present form the approximation technique presented in this paper is only adapted to estimation problems over a simple one-dimensional parameter space. This is due to the difficulty in the interpretation of level crossings for multidimensional surfaces. We are currently developing generalizations of the technique to two dimensions by modeling of the local maxima with a two-dimensional Poisson field.

Appendix I

Here we derive expressions (29) and (30) by application of the maximal and uniform probability models $\{P_i^1\}$ and $\{P_i^2\}$ described in Tables II and III of Section III to the upper bound on the large-error mse:

$$E\left\{\sum_{k=0}^{N+1}(w_k-D)^2P_k\right\} \tag{I.1}$$

where for convenience $N \triangleq N(D_M)$. As in Section II, define the random variables $I_1 \triangleq I[\Delta R(-D_M)\geq 0]$ and $I_2 \triangleq I[\Delta R(D_M)\geq 0]$. Also, define the conditional expectations

$$E_{ij}\{X\} \triangleq E\{X|I_1=i,\, I_2=j\} \tag{I.2}$$

where X is a random variable. Partial expansion of the expectation (I.1) yields

$$E\left\{\sum_{k=0}^{N+1}(w_k-D)^2P_k\right\} = \sum_{i,j=0,1}E_{ij}\left\{\sum_{k=0}^{N+1}(w_k-D)^2P_k\right\} \cdot P(I_1=i,\, I_2=j). \tag{I.3}$$

We next treat the maximal and the uniform models separately.

Maximal Model: $P_k = P_k^1$

Reference to Table II, Section III, gives

$$E_{00}\left\{\sum_{k=0}^{N+1}(w_k-D)^2P_k^1\right\} = E_{00}\left\{\max_{j=1,N}(w_j-D)^2I[N>0]\right\} \tag{I.4}$$

$$E_{01}\left\{\sum_{k=0}^{N+1}(w_k-D)^2P_k^1\right\} = (D_M-D)^2P_{01}(N=0) + E_{01}\left\{\max_{j=1,N+1}(w_j-D)^2I[N>0]\right\} \tag{I.5}$$

$$E_{10}\left\{\sum_{k=0}^{N+1}(w_k-D)^2P_k^1\right\}=(D_M+D)^2P_{10}(N=0)+E_{10}\left\{\max_{j=0,N}(w_j-D)^2I[N>0]\right\} \quad (I.6)$$

$$E_{11}\left\{\sum_{k=0}^{N+1}(w_k-D)^2P_k^1\right\}=\max\{(D_M+D)^2,(D_M-D)^2\}. \quad (I.7)$$

In (I.4)–(I.7) we have used the identity $\max_{j=p,p+1,\cdots,q}(w_j-D)^2 = \max_{j=p,q}(w_j-D)^2$ (recall monotonicity of $\{w_j\}$), and the conditional probabilities $P_{ij}(A)=E_{ij}\{I[A]\}$ have been defined.

Using the fact $(w_j-D)^2 \geq (w_k-D)^2$ iff $w_j+w_k\leq 2D$,

$$\begin{aligned}E_{00}&\left\{\max_{j=1,N}(w_j-D)^2I[N>0]\right\}\\&=E_{00}\{(w_1-D)^2I[N=1]\}\\&\quad+E_{00}\{(w_1-D)^2I[w_1+w_N\leq 2D]I[N>0]\}\\&\quad+E_{00}\{(w_N-D)^2I[w_1+w_N>2D]I[N>0]\}.\end{aligned} \quad (I.8)$$

Likewise,

$$\begin{aligned}E_{01}&\left\{\max_{j=1,N+1}(w_j-D)^2I[N>0]\right\}\\&=E_{01}\{(w_1-D)^2I[w_1<2D-D_M]I[N>0]\}\\&\quad+(D_M-D)^2P_{01}(N>0,\ w_1>2D-D_M)\end{aligned} \quad (I.9)$$

and

$$\begin{aligned}E_{10}&\left\{\max_{j=0,N}(w_j-D)^2I[N>0]\right\}\\&=E_{10}\{(w_N-D)^2I[w_N>2D+D_M]I[N>0]\}\\&\quad+(D_M+D)^2P_{10}(N>0,\ w_N<2D+D_M).\end{aligned} \quad (I.10)$$

We now specialize to the case $D>0$. The case $D\leq 0$ follows analogously. For $D>0$, under the positive delay hypothesis the following expression is easily derived via (I.8):

$$\begin{aligned}E_{00}&\left\{\sum_{k=0}^{N+1}(w_k-D)^2P_k^1\right\}\\&=\int_D^{D_M}(\tau-D)^2\\&\quad\cdot P_{00}(w_N\in[\tau,\tau+d\tau],\ N(-D_M,2D-\tau)=0)\\&\quad+\int_{2D-D_M}^{D}(\tau-D)^2\\&\quad\cdot P_{00}(w_1\in[\tau,\tau+d\tau],\ N(2D-\tau,D_M)=0)\\&\quad+\int_{-D_M}^{2D-D_M}(\tau-D)^2\\&\quad\cdot P_{00}(w_1\in[\tau,\tau+d\tau]).\end{aligned} \quad (I.11)$$

Analogously, (I.9) and (I.10) give simple expressions for (I.6) and (I.7):

$$\begin{aligned}E_{01}&\left\{\sum_{k=0}^{N+1}(w_k-D)^2P_k^1\right\}\\&=(D_M-D)^2P_{01}(N(-D_M,2D-D_M)=0)\\&\quad+\int_{-D_M}^{2D-D_M}(\tau-D)^2P_{01}(w_1\in[\tau,\tau+d\tau])\end{aligned} \quad (I.12)$$

$$E_{10}\left\{\sum_{k=0}^{N+1}(w_k-D)^2P_k^1\right\}=(D_M+D)^2. \quad (I.13)$$

Substitution of (I.11)–(I.13) and (I.7) into (I.3) gives the final result

$$E\left\{\sum_{k=0}^{N+1}(w_k-D)^2P_k^1\right\}=\int_{-D_M}^{D_M}(\tau-D)^2h_0(\tau)\,d\tau+(D_M-D)^2\alpha_D+(D_M+D)^2\beta_D \quad (I.14)$$

where for $D>0$,

$$h_D(\tau)\triangleq\begin{cases}P_{00}(N(-D_M,2D-\tau)=0,\ dN(\tau)>0,\ N(\tau,D_M)=0)E\{(1-I_1)(1-I_2)\}, & \tau>D\\ P_{00}(N(-D_M,\tau)=0,\ dN(\tau)>0,\ N(2D-\tau,D_M)=0)E\{(1-I_1)(1-I_2)\}, & 2D-D_M<\tau\leq D\\ P(N(-D_M,\tau)=0,\ dN(\tau)>0|I_1=0)E\{1-I_1\}, & \tau\leq 2D-D_M\end{cases}$$

$$\alpha_D=\exp\left(-\int_{-D_M}^{2D-D_M}\lambda_{01}(\tau)\,d\tau\right)E\{(1-I_1)I_2\}$$

$$\beta_D=E\{I_1\}. \quad (I.15)$$

A similar analysis for $D\leq 0$ yields (I.14) with

$$h_D(\tau)\triangleq\begin{cases}P_{00}(N(-D_M,\tau)=0,\ dN(\tau)>0,\ N(2D-\tau,D_M)=0)E\{(1-I_1)(1-I_2)\}, & \tau\leq D\\ P_{00}(N(-D_M,2D-\tau)=0,\ dN(\tau)>0,\ N(\tau,D_M)=0)E\{(1-I_1)(1-I_2)\}, & D<\tau\leq 2D+D_M\\ P(dN(\tau)>0,\ N(\tau,D_M)=0|I_2=0)E\{1-I_2\}, & \tau>2D+D_M\end{cases}$$

$$\alpha_D\triangleq E\{I_2\}$$

$$\beta_D\triangleq\exp\left(-\int_{2D+D_M}^{D_M}\lambda_{10}(\tau)\,d\tau\right)E\{I_1(1-I_2)\}. \quad (I.16)$$

Specialization of (I.14) to the case $D=0$ gives

$$E\left\{\sum_{k=0}^{N+1} w_k^2 P_k^1\right\} = \int_{-D_M}^{D_M} \tau^2 h_0(\tau)\, d\tau + D_M^2(1-P(I_1=0,\, I_2=0)). \quad \text{(I.17)}$$

Uniform Model $P_k = P_k^2$

Reference to Table III, Section II, gives

$$E_{00}\left\{\sum_{k=0}^{N+1}(w_k-D)^2 P_k^2\right\} = E_{00}\left\{\frac{1}{N}\sum_{k=1}^{N}(w_k-D)^2 I[N>0]\right\} = \sum_{n=1}^{\infty}\frac{1}{n}\sum_{k=1}^{n}\int_{-D_M}^{D_M}(\tau-D)^2 P_{00}(w_k\in[\tau,\tau+d\tau)) \quad \text{(I.18)}$$

$$E_{01}\left\{\sum_{k=0}^{N+1}(w_k-D)^2 P_k^2\right\} = E_{01}\left\{\frac{1}{N+1}\sum_{k=1}^{N+1}(w_k-D)^2\right\} = \sum_{n=1}^{\infty}\frac{1}{n+1}\sum_{k=1}^{n}\int_{-D_M}^{D_M}(\tau-D)^2 P_{01}(w_k\in[\tau,\tau+d\tau)) + (D_M-D)^2\sum_{n=0}^{\infty}\frac{1}{n+1}P_{01}(N=n) \quad \text{(I.19)}$$

$$E_{10}\left\{\sum_{k=0}^{N+1}(w_k-D)^2 P_k^2\right\} = E_{10}\left\{\frac{1}{N+1}\sum_{k=0}^{N}(w_k-D)^2\right\} = \sum_{n=1}^{\infty}\frac{1}{n+1}\sum_{k=1}^{n}\int_{-D_M}^{D_M}(\tau-D)^2 P_{10}(w_k\in[\tau,\tau+d\tau)) + (D_M+D)^2\sum_{n=0}^{\infty}\frac{1}{n+1}P_{10}(N=n) \quad \text{(I.20)}$$

$$E_{11}\left\{\sum_{k=0}^{N+1}(w_k-D)^2 P_k^2\right\} = E_{11}\left\{\frac{1}{N+2}\sum_{k=0}^{N+1}(w_k-D)^2 P_k^2\right\} = \sum_{n=1}^{\infty}\frac{1}{n+2}\sum_{k=1}^{n}\int_{-D_M}^{D_M}(\tau-D)^2 P_{11}(w_k\in[\tau,\tau+d\tau)) + \left[(D_M+D)^2+(D_M-D)^2\right]\sum_{n=0}^{\infty}\frac{1}{n+2}P_{11}(N=n). \quad \text{(I.21)}$$

Substitution of (I.18)–(I.21) into (I.3) yields

$$\begin{aligned} E\left\{\sum_{k=0}^{N+1}(w_k-D)^2 P_k^2\right\} &= \int_{-D_M}^{D_M}(\tau-D)^2\sum_{n=1}^{\infty}\sum_{k=1}^{n}\Big[\frac{1}{n}P_{00}(w_k\in[\tau,\tau+d\tau)) \cdot E\{(1-I_1)(1-I_2)\} \\ &\quad + \frac{1}{n+1}P_{01}(w_k\in[\tau,\tau+d\tau))E\{(1-I_1)I_2\} \\ &\quad + \frac{1}{n+1}P_{10}(w_k\in[\tau,\tau+d\tau))E\{I_1(1-I_2)\} \\ &\quad + \frac{1}{n+2}P_{11}(w_k\in[\tau,\tau+d\tau))E\{I_1I_2\}\Big] \\ &\quad + (D_M-D)^2\sum_{n=0}^{\infty}\Big[\frac{1}{n+1}P_{01}(N=n)E\{(1-I_1)I_2\} + \frac{1}{n+2}P_{11}(N=n)E\{I_1I_2\}\Big] \\ &\quad + (D_M+D)^2\sum_{n=0}^{\infty}\Big[\frac{1}{n+1}P_{10}(N=n)E\{I_1(1-I_2)\} + \frac{1}{n+2}P_{11}(N=n)E\{I_1I_2\}\Big]. \end{aligned} \quad \text{(I.22)}$$

Equation (I.22) is next transformed to an inequality by using the trivial inequalities

$$\frac{1}{n+2}<\frac{1}{n+1}<\frac{1}{n}$$

for $n>0$ and identifying

$$P(w_k\in[\tau,\tau+d\tau)) = a_{k-1,n-k}(\tau)\rho(\tau)\,d\tau \quad \text{(I.23)}$$

where

$$\begin{aligned} a_{k-1,n-k}(\tau) &\triangleq P\big(N(\tau-D_M,\tau)=k-1,\; N(\tau,D_M)=n-k \,|\, dN(\tau)>0\big) \\ \rho(\tau)d\tau &\triangleq P(dN(\tau)>0). \end{aligned} \quad \text{(I.24)}$$

This yields the upper bound

$$E\left[\sum_{k=0}^{N+1}(w_k-D)^2P_k^2\right] \le \int_{-D_M}^{D_M}(\tau-D)^2\rho(\tau)\sum_{n=1}^{\infty}\frac{1}{n}\sum_{k=1}^{n}a_{k-1,n-k}(\tau)\,d\tau + \alpha_2(D_M-D)^2+\beta_2(D_M+D)^2 \quad \text{(I.25)}$$

where α_2, β_2 are given by

$$\alpha_2 = \sum_{n=0}^{\infty}\frac{1}{n+1}P(N=n|I_2=1)E\{I_2\} \quad \text{(I.26)}$$

$$\beta_2 = \sum_{n=0}^{\infty}\frac{1}{n+1}P(N=n|I_1=1)E\{I_1\}. \quad \text{(I.27)}$$

Appendix II

We give expressions for the conditional and unconditional intensities ρ and ρ_{0^*} of the level crossing process $N \triangleq \{N(\tau)\}$, defined in (9), over the interval $\tau \in [-D_M, 0)$, for $D = 0$, and under the approximation $\Delta R = \hat{R}_{12}(\tau) - \hat{R}_{12}(0)$ discussed in Section V. For $D = 0$ the intensity of N over the foregoing region for τ is the intensity of the zero up crossings by the Gaussian random process $X = \Delta R$. The intensity of Gaussian-generated up crossing processes has been extensively studied, and we follow the development in [12] for the following.

Proposition 1

Let $x(\tau)$ be an almost surely continuous Gaussian process with mean $\mu(\tau)$, variance $\sigma(\tau)$, and covariance $\sigma(\tau, v)$. Let $r_{ij}(r,v) = \partial^{i+j}/\partial\tau^i\partial v^j\,\sigma(\tau,v)(r_{00} \triangleq \sigma)$, and assume the derivatives

$$\dot{\mu}(\tau), \quad r_{10}(\tau,\tau), \quad r_{10}(\tau,t_0), \quad r_{01}(t_0,\tau), \quad r_{11}(\tau,\tau)$$

are continuous in τ. Then if the matrix

$$\Lambda = \begin{bmatrix} r_{00}(\tau,\tau) & r_{01}(\tau,\tau) & r_{00}(\tau,t_0) \\ r_{10}(\tau,\tau) & r_{11}(\tau,\tau) & r_{10}(\tau,t_0) \\ r_{00}(t_0,\tau) & r_{01}(t_0,\tau) & r_{00}(t_0,t_0) \end{bmatrix} \tag{II.1}$$

is positive definite, the following holds. The intensity function of the number of zero up crossings by x over $[t_0, t]$ given $x(t_0) < 0$ is

$$\rho_{0^*}(\tau) = K_1 \int_0^\infty y\Phi(a_0 y + a_1)\exp\left\{-\frac{1}{2}(y+a_2)^2\right\} dy \tag{II.2}$$

and

$$K_1(\tau) = \frac{1}{\sqrt{c}\, d_3 |\Lambda|} \frac{1}{\Phi\left(\dfrac{-\mu(t_0)}{\sqrt{r_{00}(t_0)}}\right)} \phi\left(\mu(\tau)\sqrt{d_1 - \frac{d_2^2}{d_3}}\right) \tag{II.3}$$

$$a_0 = \frac{b_2}{\sqrt{d_3 c}} \tag{II.4}$$

$$a_1 = \left[-\mu(t_0) + \frac{b_1\mu(\tau)}{c} - b_2\eta(\tau)\right]\sqrt{c} \tag{II.5}$$

$$a_2 = -\left[\eta(\tau) + \frac{d_2}{d_3}\mu(\tau)\right]\sqrt{d_3} \tag{II.6}$$

where in (II.3)–(II.6) the quantities d_i and b_i are implicitly defined in terms of Λ^{-1}:

$$\Lambda^{-1} = \begin{bmatrix} A & b \\ b^T & c \end{bmatrix} \tag{II.7}$$

$$\begin{bmatrix} d_1 & d_2 \\ d_2 & d_3 \end{bmatrix} = A - \frac{1}{c} bb^T \tag{II.8}$$

$$\begin{bmatrix} b_1 \\ b_2 \end{bmatrix} = b. \tag{II.9}$$

Furthermore, the unconditional intensity function ρ is given by [12]

$$\rho(\tau) = K_2\phi(a_3)[\phi(a_4) + a_4\Phi(a_4)] \tag{II.10}$$

where

$$K_2 = \sqrt{(1-\nu_\tau^2)\frac{r_{11}(\tau)}{r_{00}(\tau)}} \qquad a_3 = \frac{\mu(\tau)}{\sqrt{r_{00}(\tau)}} \tag{II.11}$$

$$a_4 = \frac{\dot{\mu}_\tau - \nu_\tau\sqrt{\dfrac{r_{11}(\tau)}{r_{00}(\tau)}}\mu(\tau)}{\sqrt{(1-\nu_\tau^2)r_{11}(\tau)}} \tag{II.12}$$

and we have defined the correlation coefficient ν_τ as

$$\nu_\tau \triangleq \frac{r_{01}(\tau)}{\sqrt{r_{00}(\tau)r_{11}(\tau)}}. \tag{II.13}$$

Although the proof of the foregoing proposition is straightforward, the details are tedious and will not be given here. The essential element is to show that the joint density function, $g_{\tau,h}(y,z)$, of $x(\tau)$ and

$$\frac{x(\tau+h) - x(\tau)}{h}$$

given $x(t_0) < 0$ satisfies the Leadbetter conditions given in [4]. Then Leadbetter's results in [12] give that the (incomplete) intensity $\rho_{0^*}(\tau)$ is equal to the definite integral $\int_0^\infty z p_\tau(0,z)\,dz$, where $p_\tau(0,z) = \lim_{h\to 0} g_{\tau,h}(0\,z)$ is the conditional joint density. The specific form (II.2) of the conditional intensity $\rho_{0^*}(\tau)$ is then obtained by manipulation of

$$\int_0^\infty z \lim_{h\to 0} g_{\tau,h}(0,z)\,dz \tag{II.14}$$

into calculable form.

The continuity conditions on the first- and second-order moments of x will be satisfied if higher order moments of the signal autospectrum G_{33} and the observation spectra G_{11} and G_{22} exist [4].

References

[1] G. C. Carter, "Time delay estimation for passive sonar signal processing," *IEEE Trans. Acoust., Speech, Signal Processing*, vol. ASSP 29, no. 3, pp. 463–470, 1981.

[2] J. P. Ianniello, "Time delay estimation via cross-correlation in the presence of large estimation errors," *IEEE Trans. Acoust., Speech, Signal Processing*, vol. ASSP-30, no. 6, pp. 998–1003, 1982.

[3] K. Scarbrough, R. J. Tremblay, and G. C. Carter, "Performance predictions for coherent and incoherent processing techniques of time delay estimation," *IEEE Trans. Acoust., Speech, Signal Processing*, vol. ASSP-31, no. 5, pp. 1191–1196, 1983.

[4] A. Hero, "Topics in time delay estimation," Ph.D dissertation, Princeton University, Princeton, NJ, ch. 5, 1984.

[5] E. Weinstein and A. J. Weiss, "Fundamental limitations in passive time delay estimation—Part II: Wide-band systems," *IEEE Trans. Acoust., Speech, Signal Processing*, vol. ASSP-32, no. 5, pp. 1064–1077, 1984.

[6] V. H. MacDonald and P. M. Schultheiss, "Optimum passive bearing estimation in a spatially incoherent noise environment," *J. Acoust. Soc. Amer.*, vol. 46, no. 1, part 1, pp. 37–43, 1969.

[7] J. P. Ianniello, E. Weinstein, and A. Weiss, "Comparison of the Ziv–Zakai lower bound on time delay estimation with correlator performance," in *ICASSP-83 Proc.*, 1983, vol. 2, pp. 875–878.

[8] J. P. Ianniello, "A discussion of the maximum likelihood estimator for two channel time delay estimation," Naval Underwater Systems Center, New London Lab., New London, CT, Tech. Memo., Apr. 1984.

[9] S. Haykin, "Radar array processing for angle of arrival estimation," *Array Signal Processing*, S. Haykin, Ed. Englewood Cliffs, NJ: Prentice-Hall, Signal Processing Series, 1985.

[10] C. H. Knapp and G. C. Carter, "The generalized correlation method for estimation of time delay," *IEEE Trans. Acoust. Speech, Signal Processing*, vol. ASSP-24, pp. 320–327, Aug. 1976.
[11] D. R. Cox and V. Isham, *Point Processes*. New York: Chapman and Hall, 1980.
[12] M. R. Leadbetter, "Point processes generated by level crossings," in *Stochastic Point Processes*, P. A. W. Lewis, Ed. New York: Wiley, 1972.
[13] I. Blake and W. C. Lindsey, "Level crossing problems for random processes," *IEEE Trans. Inform. Theory*, vol. 19, pp. 295–315, 1973.
[14] J. Abrahams, "A survey of recent progress on level crossing problems for random processes," Office of Naval Research, Tech. Memo., June 21, 1983.
[15] M. R. Leadbetter, G. Lindgren, and H. Rootzen, *Extremes and Related Properties of Random Sequences and Processes*. New York: Springer-Verlag, 1982.
[16] M. Jacobsen, *Statistical Analysis of Counting Processes*. New York: Springer-Verlag, 1982.
[17] E. Wong, *Stochastic Processes in Information and Dynamical Systems*. New York: Kreiger, 1979.
[18] A. O. Hero and S. C. Schwartz, "Level crossing representations, Poisson asymptotics and approximations to passive arrays," in *Stochastic Processes in Underwater Acoustics*, C. Baker, Ed. New York: Springer-Verlag, 1986.
[19] W. R. Hahn, "Optimum signal processing for passive sonar range and bearing estimation," *J. Acoust. Soc. Amer.*, vol. 58, no. 1, pp. 201–207, 1975.
[20] M. M. Rao, *Probability Theory with Applications*. Orlando, FL: Academic, 1984.
[21] E. Weinstein and A. J. Weiss, "Fundamental limitations in passive time delay estimation—Part I: Narrow-band systems," *IEEE Trans. Acoust., Speech, Signal Processing*, vol. ASSP-31, no. 2, pp. 472–486, Apr. 1983.